EXPERIMENTAL AND NUMERICAL STUDY OF FLOW DEFLECTION EFFECTS ON ELECTRONIC AIR-COOLING

Ahlem ARFAOUI[1,2,*], Mourad REBAY[1], Rejeb BEN MAAD[2] , Mahmoud HAMMAMI[2] and Jacques PADET[1]

[1] laboratoire UTAP-Thermomécanique, Faculté des sciences, BP 1039, 51687 Reims, France

[2] Laboratoire d'Energétique et Transferts Thermique et Massique, Faculté des sciences, 2092 Manar II, Tunisie

[*] (Corresponding Author: ahlem.arfaoui@etudiant.univ-reims.fr)

This work present a numerical and experimental investigation of the influence of transversal flow deflector on the cooling of a heated block mounted on a flat plate. The deflector is inclined and therefore it guides the air flow to the upper surface of the block. This situation is simulating the air-cooling of a rectangular integrated circuit or a current converter mounted on an electronic board. The electronic component are assumed dissipating a low or medium heat flux (with a density lower than 5000 W/m²), as such the forced convection air cooling without fan or heat sink is still sufficient. The study details the effects of the angle of deflector on the temperature and the heat transfer coefficient along the surface of the block and around it. The results of the numerical simulations and the InfraRed camera measurements show that the deviation caused by deflector may significantly enhance the heat transfer on the top face of block.

INTRODUCTION

The need for more efficient air-cooling techniques in low electric or electronic components has become the subject of increasing research in heat transfer and flow characterisation in the last two decades.

Kakaç et al. [1994] studied different cooling techniques to obtain heat transfer enhancement including the traditional methods of natural and forced convective cooling. The natural convection is used for low power electronic components. However, It is well known that cooling of high power and large scale equipment requires higher heat dissipation, that's why the forced convection is the most appropriate. High heat dissipation components are almost cooled more efficient methods, such as direct or indirect liquid cooling (immersion fluorocarbons, water …) or phase changes [Kadangode and Mason 2003].

Although, the cooling of such components is often with liquid flow or change phase, the cooling air flow is still widely used. Air cooling is the traditionally method of cooling technology due to its availability in desired amounts, low cost, easy maintenance and high reliability.

Fans are traditionally used for expelling warm air inside an electronic enclosure and racks, but there are numerous reasons why fans are undesired, including noise, vibration and the need of large spaces in the racks of servers or computers [Stewart and Stiver 2004].

The present pepr proposes to implement deflectors that guide the air flow to the most critical areas on a flat heat dissipating component when there is not enough of space to introduce heat sinks fins or a fan on the component. We study here the influence of deflectors and the inclination angle on the enhancement of heat transfer.

EXPERIMENTAL SET-UP

Figure 1 shows the physical geometry considered in this study. A flat plate is placed in a laminar air flow. On this plate is mounted a PVC module of 50x50mm and 5mm in height. A wire resistor is implanted behind the module to ensure his heating. Upon the surface of the module, a deflector of 10x1.5 x2mm is positioned and maintained with supports attached to the plate. This geometry simulates an air-cooling of a rectangular integrated circuits or current converter component mounted on an electronic board. The influence of the inclination angle of a transversal deflector has been studied by varying the angle from $\alpha = 0$, $\alpha = 10$, $\alpha = 20$, $\alpha = 30$ and $\alpha = 40°$ (Figure 1).

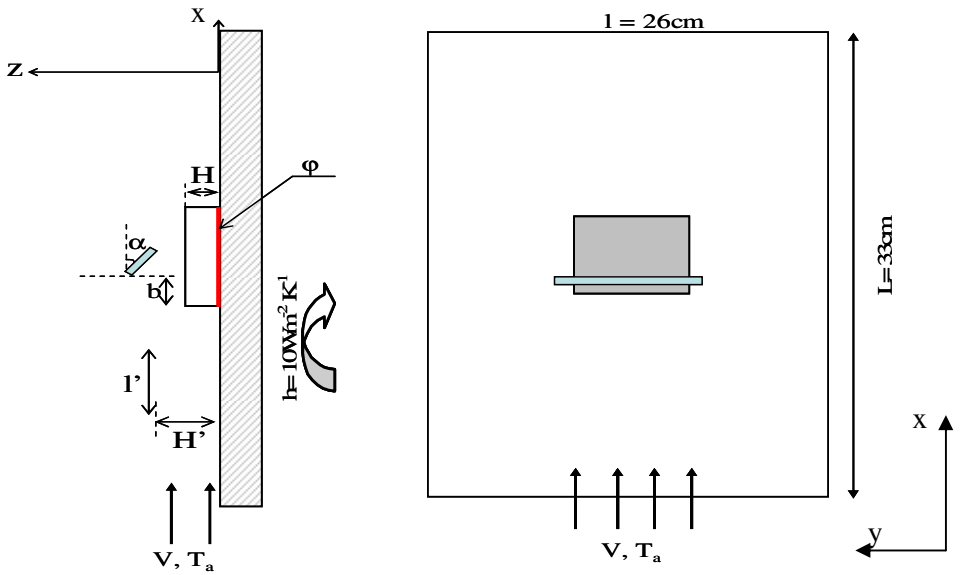

Figure 1: Experimental set-up

The experimental set-up is schematized on Figure 2. The flat plate (1) was maintained vertically at the outlet of a rectangular channel (2) with 300x100 cross flow section. On this plate is mounted a PVC module (3) of 50x50mm and 5mm in height. A wire resistor is implanted behind the module to ensure his heating. In front of surface of module, a deflector (4) of 10x1.5 x2mm is positioned and maintained with supports attached to the plate. Al-Cr thermocouples are used to measure the temperature of the bloc. The thermal cartographies of the surface temperature on the plate and heated module are obtained by a short wave InfraRed Camera.
The air flow is generated by a blower (5), in which a flow calming section is located at the 500mm of plate. Al-Cr thermocouples are used to measure the temperature of the module. The thermal cartographies were obtained by Infrared Camera (6) with Sterling circle cooling (FLIR SC1000).
The infrared thermal imaging system (FLIR, SC1000) has a range of temperature measurement from -40 °C to 1500 °C with ± 2% accuracy. The camera has a matrix with 256x256 pixels uncooled focal plane array detector operated over the wavelength range from 3.4 µm to 5 µm. Images are transferred to a computer in almost real time and stored therein for further analysis.

A wire anemometer with constant temperature regulation was used to explore the voltage signals corresponding to the flow velocity. In addition, a wire anemometer with constant current regulation was used to measure the flow temperature in typical locations from and along the

surface of the heated bloc. In order to ovoid the disturbances of flow by the anemometers, the formers (7) are introduced vertically, as such, the sensitive part of the anemometer (the wire) has been maintained perpendicular to the ascending flow. Furthermore, in order to explore temperature and velocity at different location across the air-flow, we have used a displacement system (8) of the probe, following 3 directions measurements. Minimal displacement in the horizontal direction is 0.1 mm against 0.2 in vertical direction. A computer equipped with a data acquisition card permits to acquire instantaneous signal values all 10 ms intervals and records the signals for further statistical processing.

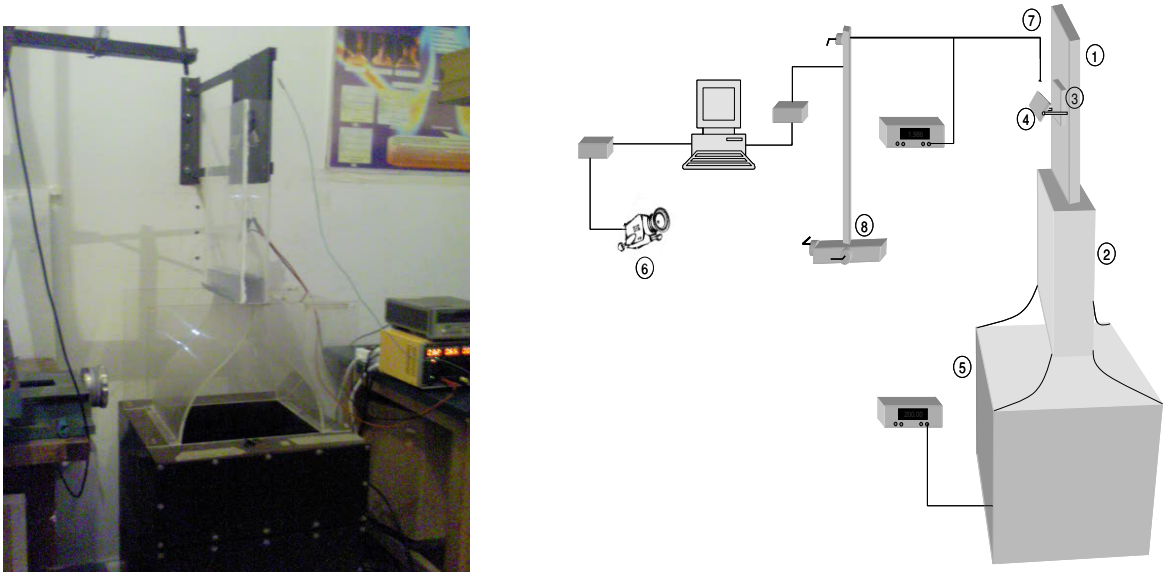

Figure 2: experimental apparatus.

EXPERIMENTAL INVESTIGATION OF THE FLOW FIELD

A fate PVC plate is placed in a laminar air flow. The flow velocity (Uair = 0.8 m/s) at the outlet section of the blower was preliminary measured by a constant temperature wire anemometer. On this plate is mounted a heated module. A wire resistor is implanted behind the module to ensure his heating. The electrical power provided to wire resistor is estimated to $\phi = 5W$. In front of surface of module, the deflector is positioned (a = 0mm) and maintained with supports attached to the plate. The details of temperature field and velocity field at surface of module and around it are acquired for different inclination angle of deflector.

Thermal cartographies To visualize the effect of inclination of deflector, an Infrared cartography of plate and hot module are represented on Figures 3 and 4.

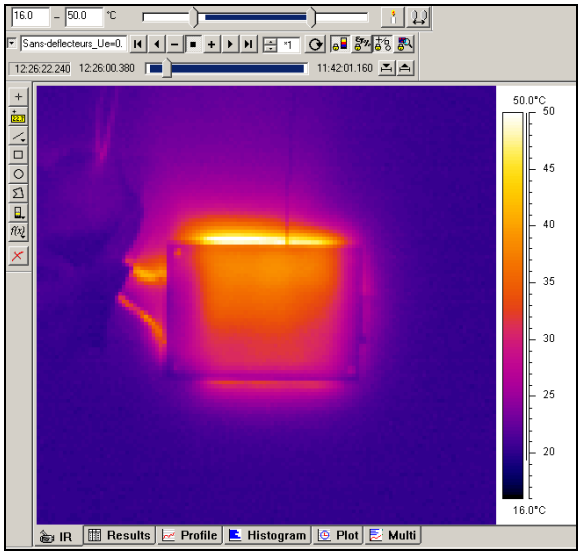

Figure 3: Infrared photography of the module mounted on PVC plane without the deflector

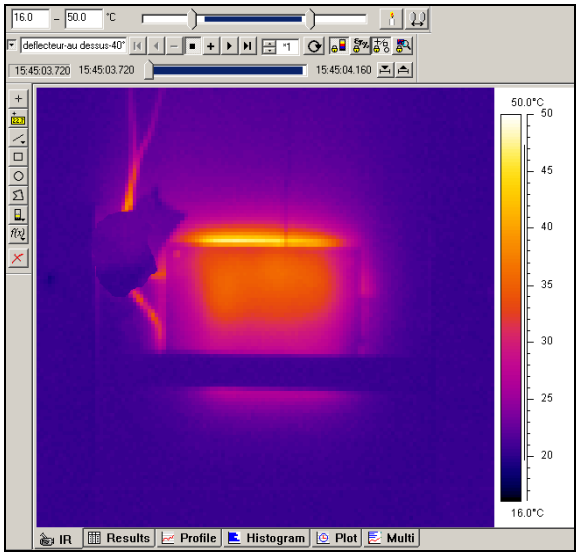

Figure 4: Infrared photography of the heated module mounted on PVC plane with the deflector

Figure 3 depicts the infrared thermal image of the top surface of the module by infrared thermography when the deflector is not introduced. The temperature gradient indicates the direction of the heat transfer in the hot module to be outward from the side and upward from the bottom. For the same flow velocity, we can note that on figure 4 that the temperature on the hot module is lower when the deflector is placed in front of its surface. The most heated zone is located from the medal of module. In addition, we note in downstream module a decrease of temperature.

Measured temperature in the fluid The axial evolutions of the measured temperature of air are plotted in Figure 5 and 6 for different positions y (perpendicular to the flow direction) above the heated module. In this paper we present evolutions on y = 2 and y = 4. The curves are given also for different inclination angle : $\alpha = 0°$, $\alpha = 10°$, $\alpha = 20°$, $\alpha = 30°$ and $\alpha = 40°$. Several behaviors can be observed from these figures. In the first zone upstream from the hot module, the temperature profile is uniform. In the second zone (near the hot module) an increase of the temperature is observed with a maxima at x = 50.

We found that the maximum evolution of the temperature was obtained at an inclination angle of 0° from x = 0mm to x = 35. However, a peak is observed in case of $\alpha = 40°$.

In figure 5, we can note two different evolutions from x = 0mm to x = 50:

- x = 0 to x = 15: axial evolution of temperature is lower at $\alpha = 40°$ than at $\alpha = 30°$, $\alpha = 20°$ and $\alpha = 10°$. We can explain these evolutions by the effect of inclination angle. Indeed, the deflector trains air flow to the surface of bloc causing contraction of thermal boundary layer.
- x = 15 to x = 50 mm: axial evolution of temperature is most important in case of $\alpha = 40°$ with a peak at x = 45 mm (27°C). The deflection of flow induces obstruction of air flow and involves the recirculation of air in front of the module. This recirculation is increasingly important that deflector's inclination is important. This causes a rise in temperature in this region.

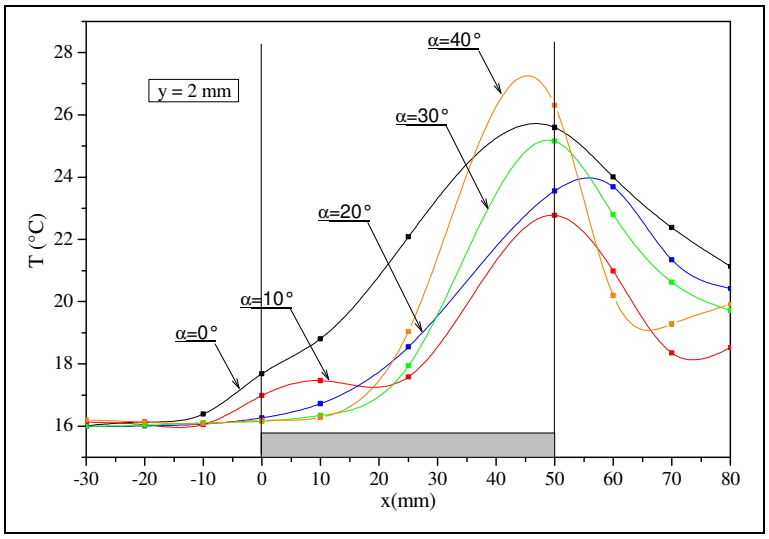

Figure 5: Comparison of axial distribution of the temperature in the air flow on y = 2mm

- For y = 4, the evolution of the temperature is higher in case of α = 40° than in case of α = 30°, α = 20° and α = 10° from x = 0 to x = 50 (Figure 6) . As, for y = 2 mm, the deflection of the flow induces obstruction of air; perturbation was created due to flow air blocked by deflectors and flow air. This causes a rise in temperature in total region.

The third zone matches with downstream of the module. One can note at y = 4 (Figure 6) that distribution of the temperature between x = 50 and x = 80 is the highest for α = 40°. The minimum is observed for α = 10°. However, on y = 2mm, the evolution of temperature significantly decreases then increases from x = 65 mm. Indeed, when the passage section between the deflector and the hot module is reduced, we note a raise of the flow temperature on the symmetry axis. But, near the left and right sides of the modules, the spacing allows air flow to escape and trains flow before encounter perturbation. The heat flux evacuated by the hot module is affected by the air flow effect that surrounds it.

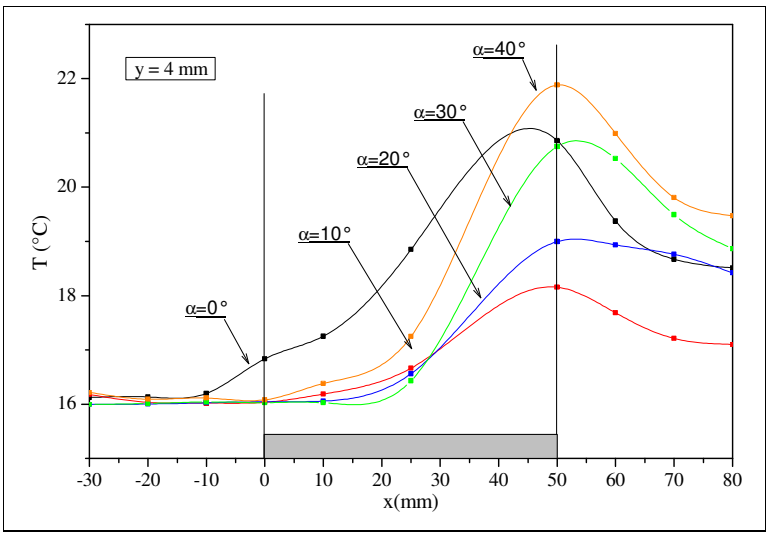

Figure 6: Comparison of axial distribution of the temperature in the air flow on y = 4mm

Thermal fluctuating field The standard deviation of the flow is given by the following expression: $I_{th} = \frac{\sqrt{\overline{T'^2}}}{T_s - T_\infty}$

Where T' is the temperature fluctuation and $T_s - T_\infty$ is the temperature difference between the module and the ambient medium.

Figures 8 and 9 present a comparison of axial distribution of the standard thermal deviations of the flow at y = 2mm and y = 4mm in cases of α = 0°, α = 10°, α = 20°, α = 30° and α = 40°.
In the case of α = 0°, the standard deviations of flow are low (I_{th} = 5%) near the vertical module. We can explain that by standardization of temperature (Figures 8 and 9). In the case of α = 10°, we note maxima (I_{th} = 27%) located at x = 25. These maxima result from the interaction of a convection flow trained by inclination of deflector and the hot air arising from a module [Zinoubi, Ben Maad 2005]. However, for α = 40° the standard deviations increase before slowly decreasing and reaching 22% at x = 50 mm. We can note tow different behaviors from x = 50 for y =2 and y =4. Indeed, for y = 2, the standard deviations of flow exhibit a maximum at x = 60, decrease suddenly at x = 70 (I_{th} = 17%) and increase immediately and reach 26 %. These maxima result from the interaction of a convection flow and the hot air escaping from the rotating rolls. These two maxima correspond to the regions where the interaction between hot air and the ambient air is the most important. At x = 70, a clear decrease is observed, so, the flow is disturbed because it receives directly a flow thread from the ambient that is influenced by the rotating rolls. The homogenization of the turbulence progresses slowly as the height increases (Figures 8 and 9). Moreover, we can note that % I_{th} is more important when α = 40° than the other cases since the recirculation is increasingly important as deflector's inclination is important.

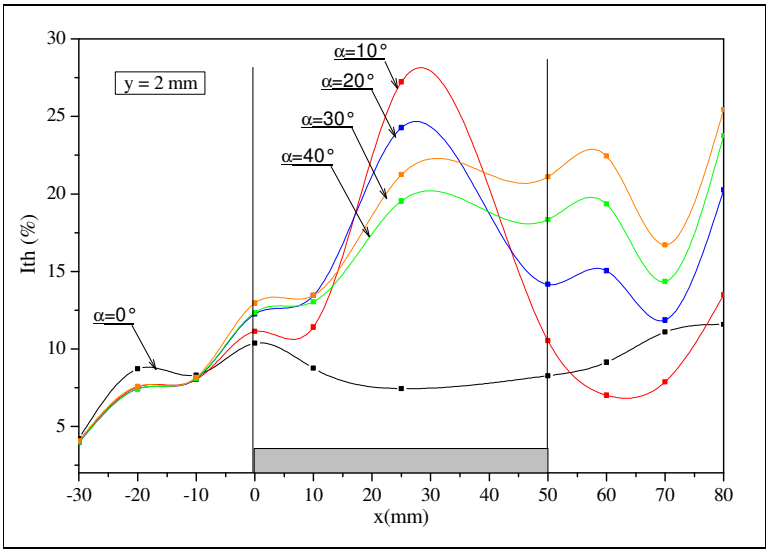

Figure 8: Comparison of axial distribution of the standard thermal deviations in the flow on y = 2mm

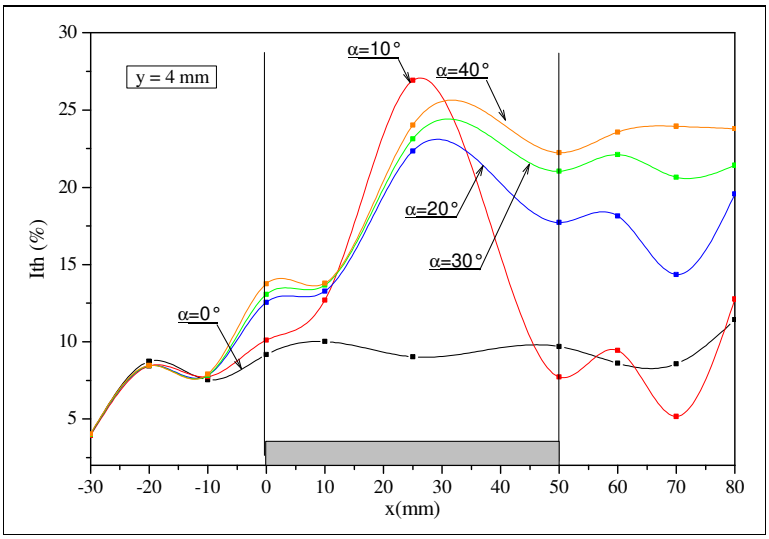

Figure 9: Comparison of axial distribution of the standard thermal deviations in the flow on y = 4mm

Thermal skewness and thermal flatness factors The investigation of the skewness and flatness factors, are respectively given by: expression: $S_{th} = \frac{\overline{T'^3}}{\left(\sqrt{\overline{T'^2}}\right)^3}$ and $F_{th} = \frac{\overline{T'^4}}{\left(\sqrt{\overline{T'^2}}\right)^4}$.

These parameters allow the comparison of the probability density function of the flow temperature fluctuations and the ideal Gaussian distribution S_{th} = 0 and F_{th} = 3. The axial distribution of the skewness and flatness factor are given in Figures 10, 11, 12 and 13.

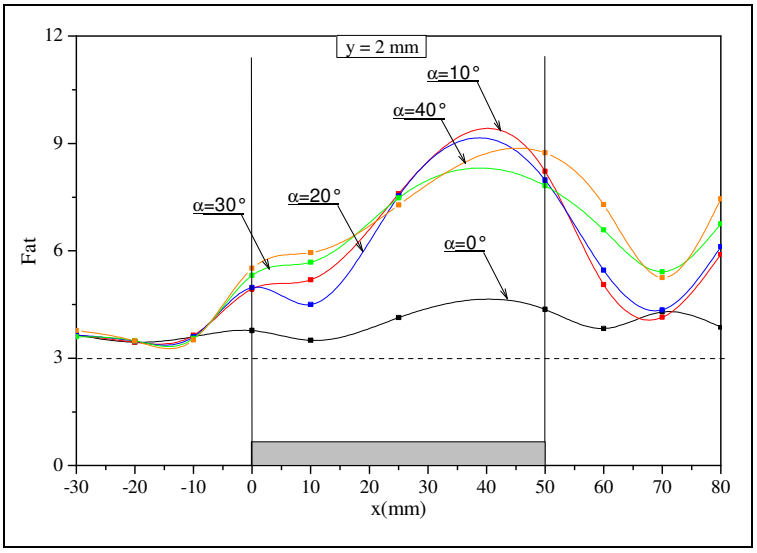

Figure 10 Comparison of axial distribution of the thermal flatness factor at y =2 mm

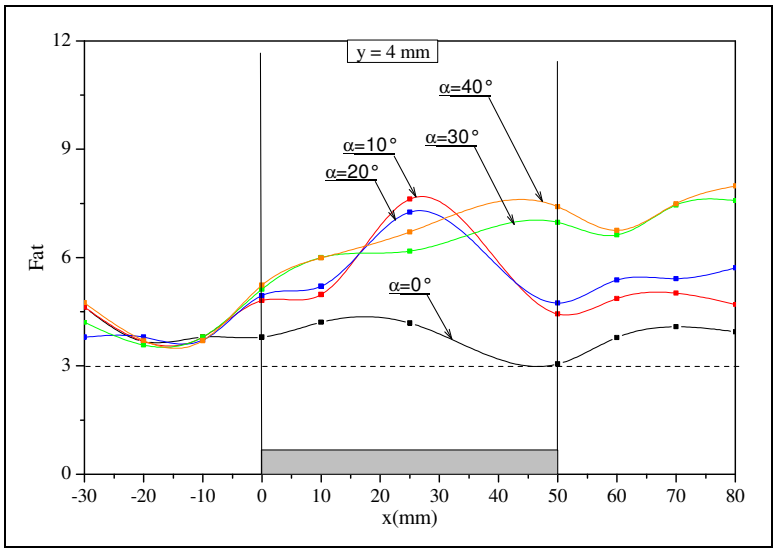

Figure 11 Comparison of axial distribution of the thermal flatness factor at y =4 mm

In case of $\alpha = 0°$, the flatness factor approaches $F_{th} = 3$ (Figures 11 and 12) and the skewness factor approaches $S_{th} = 0$ (Figures 12 and 13). Consequently, it is deduced that in this region, the probability density governing the temperature fluctuations in the flow follows approximately the ideal Gaussian distribution. The zero value of the skewness factor indicates an equal probability of the presence of the hot air coming from the module and the ambient air.

For the other cases, the flatness factor is higher than $F_{th} = 3$ in every side of axis (Figures 10 and 11). Thus, it is deduced that in this region, the air flow governs. The skewness factor confirms this hypothesis. The negative skewness factor, characterize a strong flow of cold air arising from the ambient media (Figures 12 and 13).

From x = 50, the flatness factor decrease and approaches $F_{th} = 3$ ($\alpha = 10°$ and $\alpha = 20°$) before increasing from x = 70. All the same, the skewness factor increase and approaches $S_{th} = 0$ ($\alpha = 10°$ and $\alpha = 20°$) before decreasing from x = 70. It can be concluded that the air is still hot in this region. For the cases of $\alpha = 30°$ and $\alpha = 40°$, it is deduced that in this region, the air flow governs.

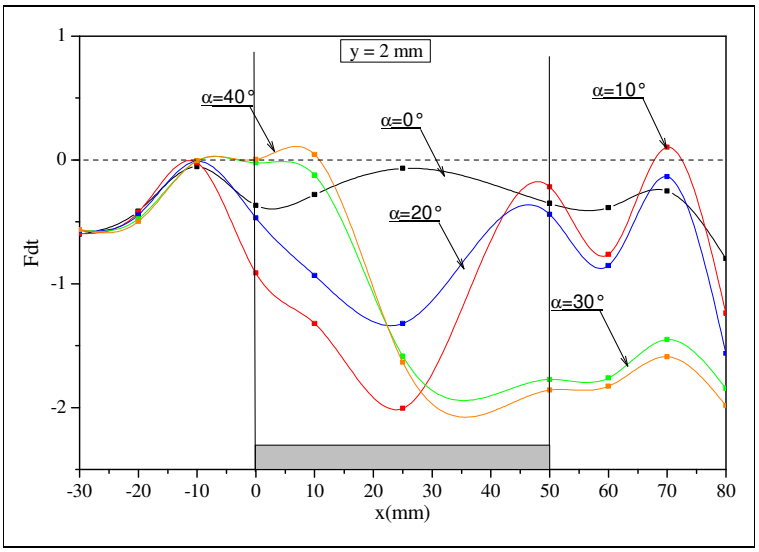

Figure 12 Comparison of axial distribution of the thermal skewness factor at y =2 mm

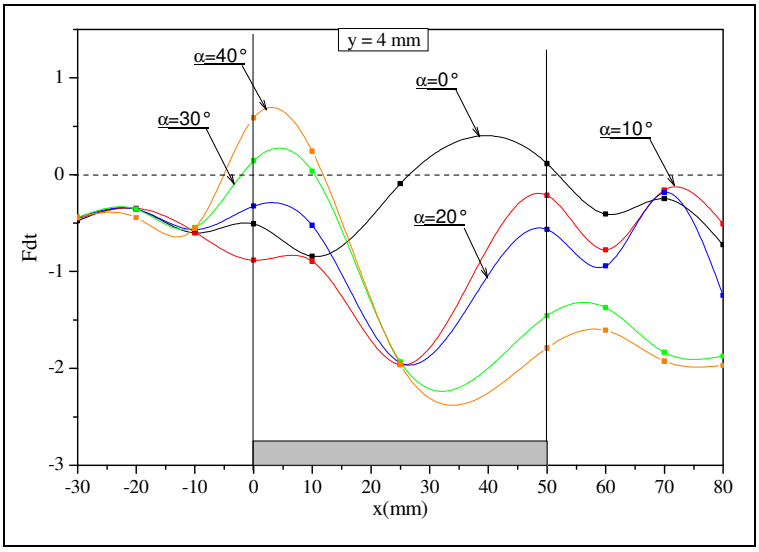

Figure 13 Comparison of axial distribution of the thermal skewness factor at y =4 mm

Dynamical field The axial evolutions of the velocity of the flow are represented in Figure 14 and 15 for different positions y near the surface of module (y =2, y = 4). This figures present a comparison of the velocity profiles in the flow for different inclination angle : $\alpha = 0°$, $\alpha = 10°$, $\alpha = 20°$, $\alpha = 30°$ and $\alpha = 40°$.

For y = 2 and y = 4, we note that the velocity profile is almost flat in case of $\alpha = 10°$ (Figures 14 and 15). However, in cases of $\alpha = 30°$ and $\alpha = 40°$, the velocity decreases significantly and approaches 0.3 m/s from x = 0. We can explain that by detachment of flow in the upstream corner of the module. Nevertheless, the profile of velocity increase from x = 0 to x = 25 before decreasing significantly. This behavior results from the inclination of deflector that blocks the air flow. The velocity profiles confirm those of temperature (Figures 5 and 6). We can observe a decrease of temperature when the velocity increase from x = 0 to x = 25.

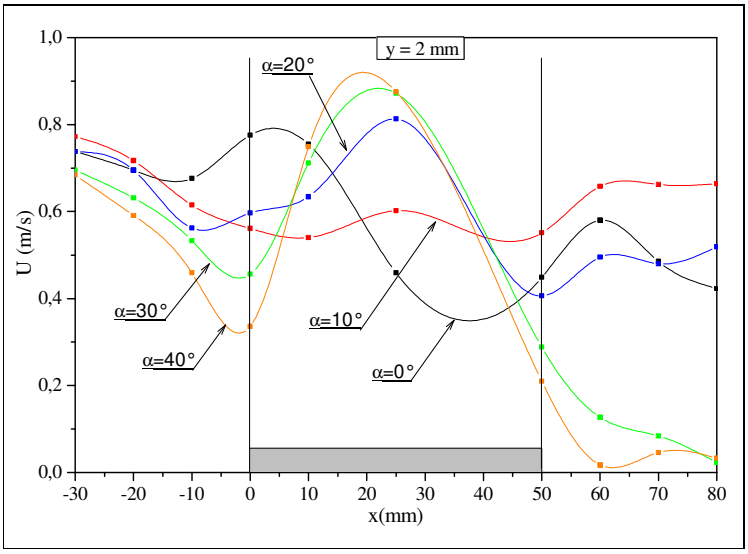

Figure 14: Comparison of axial distribution of velocity at y = 2mm

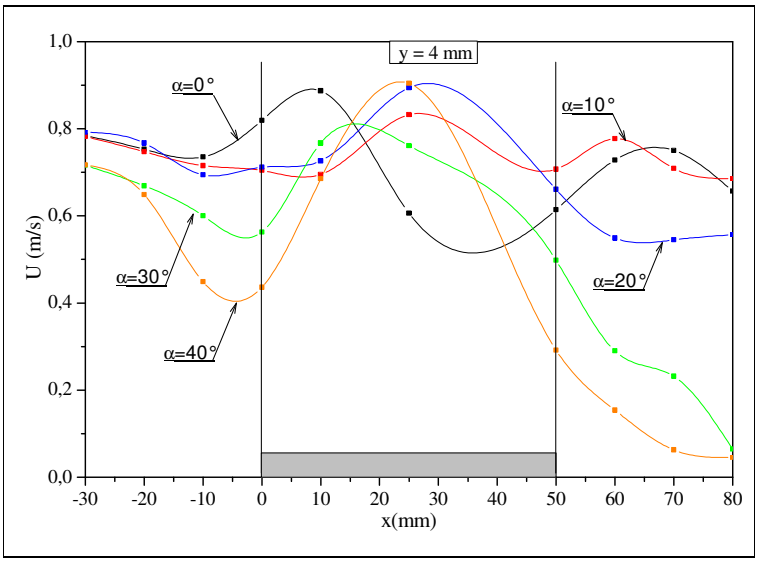

Figure 15: Comparison of axial distribution of velocity at y = 2mm

Dynamical fluctuating field The standard dynamic deviation of the flow is given by the following expression: $I_d = \frac{\sqrt{\overline{U'^2}}}{U_e}$. Figures 16 and 17 present the standard dynamic deviation of the flow for y = 2 and y = 4.

For y =2, the effect of inclination angle is noted from x = 10. Moreover, in case of α = 10°, $\%I_d$ steels flat ($\%I_d$ = 27%) from x = 10 to x = 50 before increases slightly. But, in case of α = 40°, $\%I_d$ decrease significantly. However, for y =4, we note a maximum for each case, for α = 10°, $\%I_d$ steels flat ($\%I_d$ = 24%) from x = 10 to x = 50 before increases slightly. In case of α = 20°,

the maximum of $\%I_d$ is obtained at x = 55. This maximum is translated in case of $\alpha = 30°$ ($\%I_{dmax} = 35\%$ at x = 40). However, in case of $\alpha = 40°$, $\%I_{dmax} = 30\%$ at x = 25.

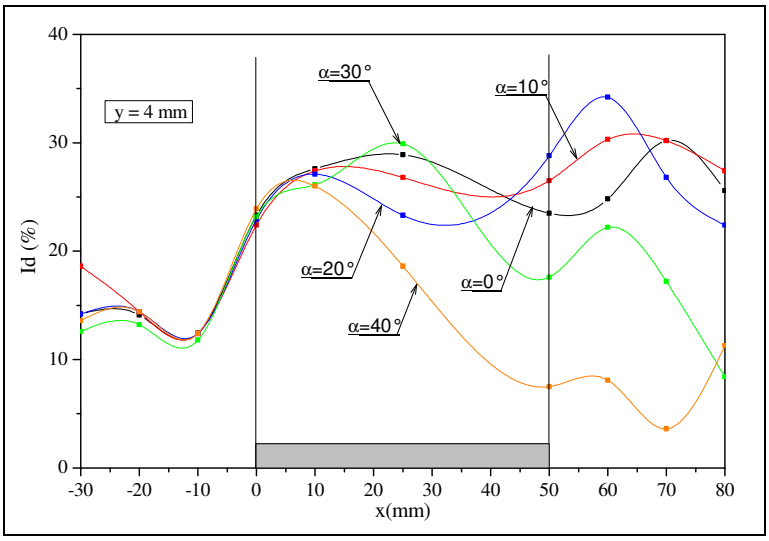

Figure 16: Comparison of axial distribution of the standard dynamical deviations of the flow at y = 2mm

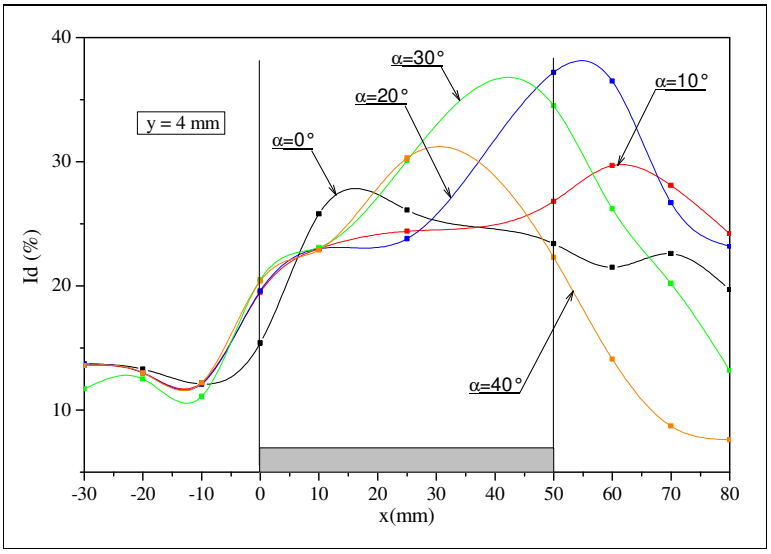

Figure 17: Comparison of axial distribution of the standard dynamical deviations of the flow at y = 4mm

Dynamical skewness and dynamical flatness factors The investigation of the skewness and flatness factors, are respectively given by: expression: $S_d = \frac{\overline{U'^3}}{\left(\sqrt{\overline{U'^2}}\right)^3}$ and $F_d = \frac{\overline{U'^4}}{\left(\sqrt{\overline{U'^2}}\right)^4}$.

These parameters allow the comparison of the probability density function of the flow velocity fluctuations and the ideal Gaussian distribution: $S_d = 0$ and $F_d = 3$. The axial distribution of the skewness and flatness factor are given in Figures 18, 19, 20 and 21 for y = 2 and y = 4.
From x = -30 to x = 0, the flatness factor approaches $F_d = 3$ (Figures 18 and 19) and the skewness factor approaches $S_d = 0$ (Figures 20 and 21). This behavior characterizes a strong flow of cold air arising from the ambient media.

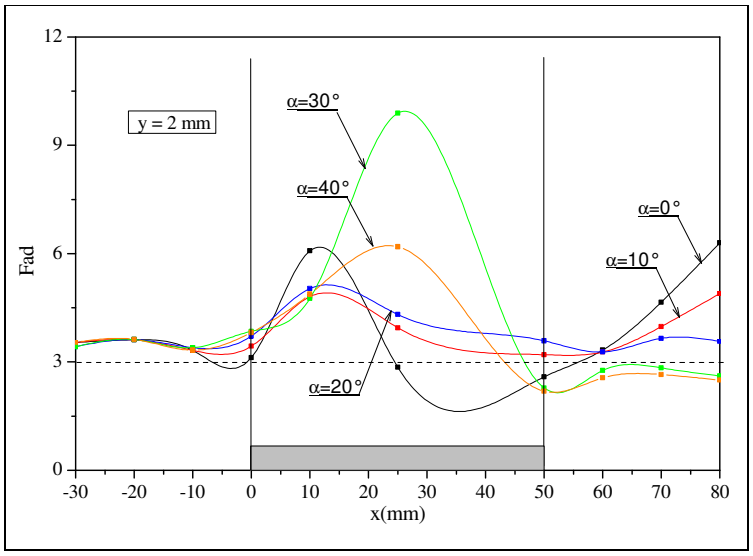

Figure 18 Comparison of axial distribution of the dynamic flatness factor at y =2 mm

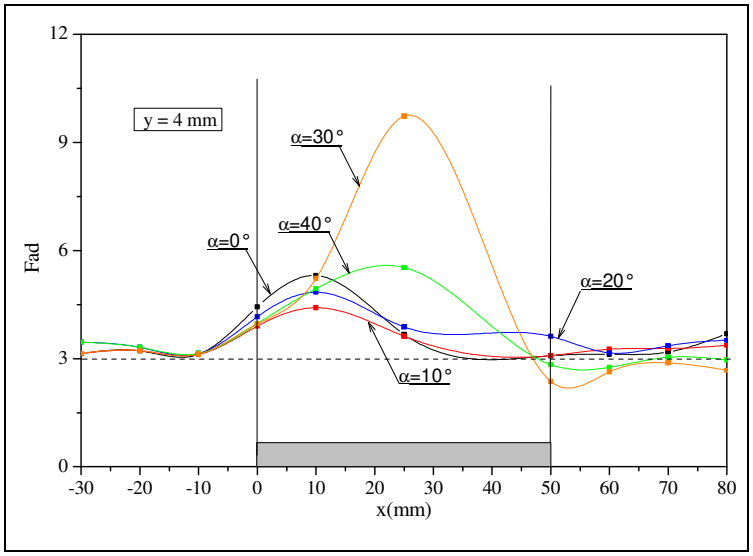

Figure 19 Comparison of axial distribution of the dynamic flatness factor at y =4 mm

In case of $\alpha = 0°$, $\alpha = 10°$, $\alpha = 20°$ (Figure 19), the flatness factor increase slightly ($F_d = 5$) at x = 10 before decreasing and approaches $F_d = 3$ as far as x = 80. However, in cases of $\alpha = 30°$, $\alpha = 40°$, we note a maximum at x = 25 ($F_d = 10$ for $\alpha = 30°$and $F_d = 6$ for $\alpha = 40°$). Thus, it is deduced that in this region, the velocity is low. The skewness factor confirms this hypothesis

(Figure 20). The negative skewness factor, characterize a flow with low velocity created by obstruction of flow due to the deflector.

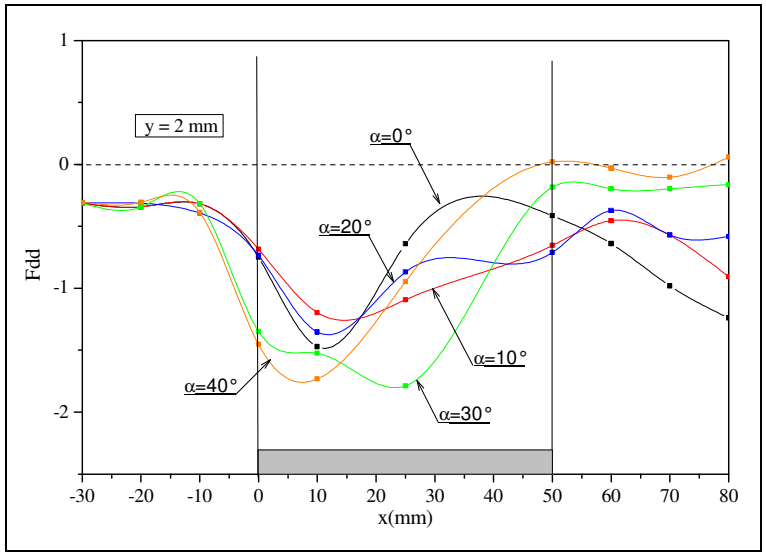

Figure 20 Comparison of axial distribution of the dynamic skewness factor at y =2 mm

For y = 12, the skewness factor is positive as far as x = 30, this behavior is the characteristics the recirculation created by subdivision of flow in presence of deflector.

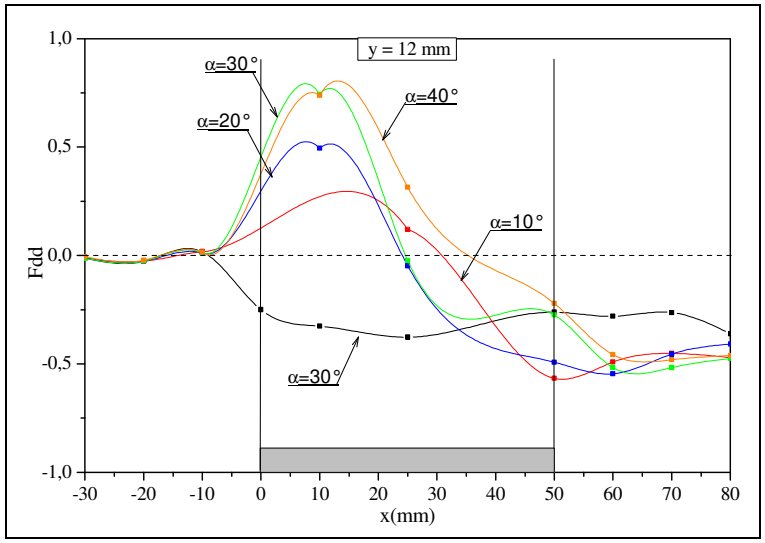

Figure 21 Comparison of axial distribution of the dynamic skewness factor at y =12 mm

NUMERICAL ANALYSIS

In order to provide additional information eventually not accessible by experiments and to predict the behavior of flow, we used a three dimensional simulation CFD code.
The software Fluent was used as a CFD tool in this study. To take advantage of the symmetry present in the problem, we have chosen half studied medium. For all calculation performed, a fine grid (110x40x40) of control volume was found to be sufficient for all cases. Quadrilateral mapped grid and paved grid were used to construct mesh. In order to check grid independence, numerical simulations of the steady problem are performed with various grid sizes.

Temperature field Figure 22 shows temperature on the surface at surface of the heated module (black rectangle) and its supporting plate for different inclination angles of the deflector: $\alpha = 0°$, $\alpha = 20$, $\alpha = 30°$ and $\alpha = 40°$.

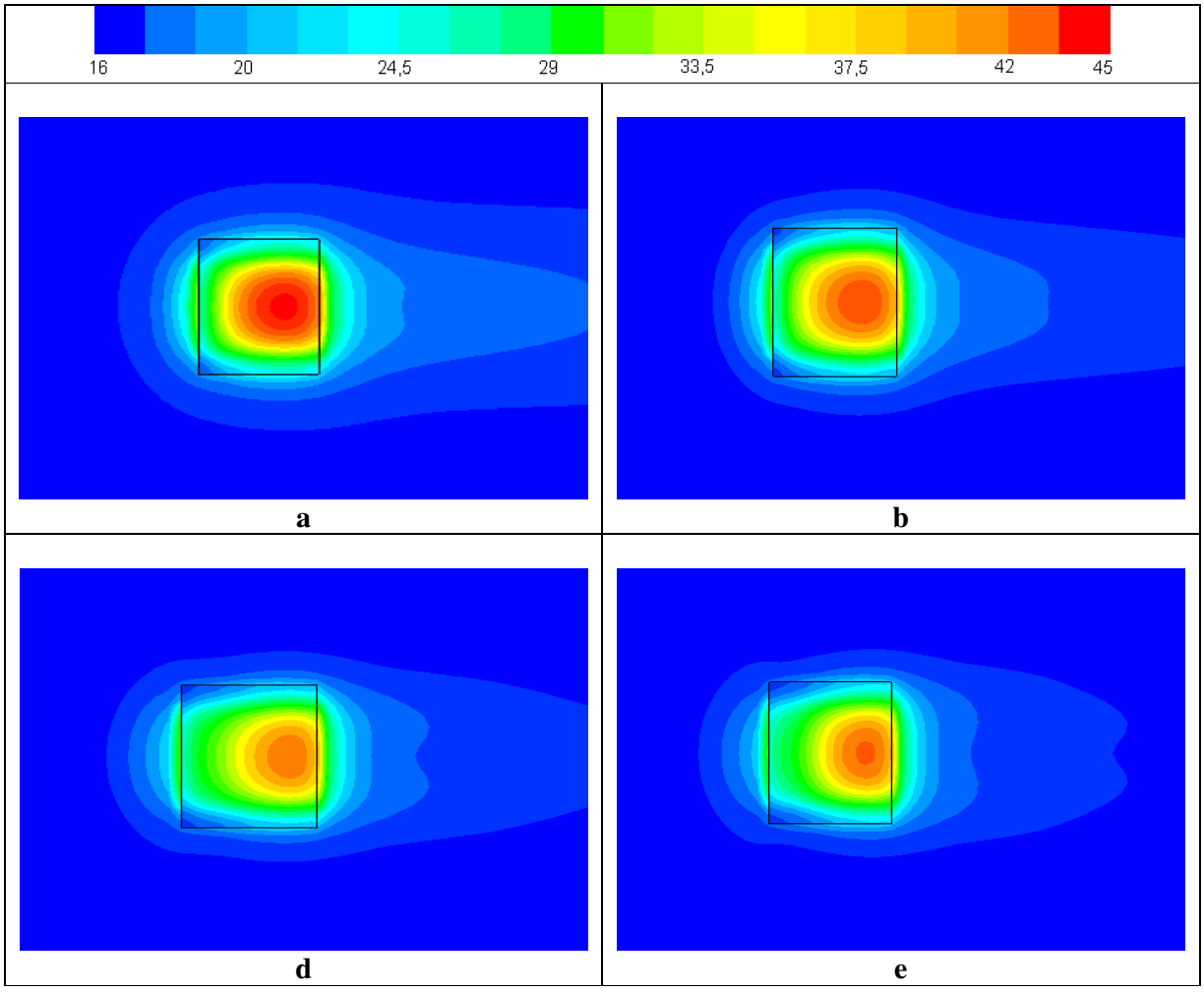

Figure 22: Isothermals in the cases of $\alpha = 0°$ (**a**), $\alpha = 20°$ (**b**) $\alpha = 30°$ (**c**) and $\alpha = 40°$ (**d**)

In case of $\alpha = 0°$, a maximum of temperature is located in the upper module (45°C), the higher temperature recovers a big region. This region becomes smaller and smaller when inclination of angle increases. But, in case of $\alpha = 40°$, some regions exhibit a rising of temperature. However, in the downstream of the module temperature of plate is the fewest. Given that the deflector in

this case blocks the air flow and causes a downstream recirculation (Figure 23-g) able to extract more heat from the surface of module and the surface of plate near the downstream corner of module. These contours

Streamlines Graphs 23 show in the figures at left the streamlines on z = 0 (midline of the width) and in figures at right the streamlines on y = -2 (3 mm up the surface of PVC plate). Figure 23 presents different inclinations of deflector: $\alpha = 0°$, $\alpha = 10°$, $\alpha = 20$, $\alpha = 30°$ and $\alpha = 40°$.

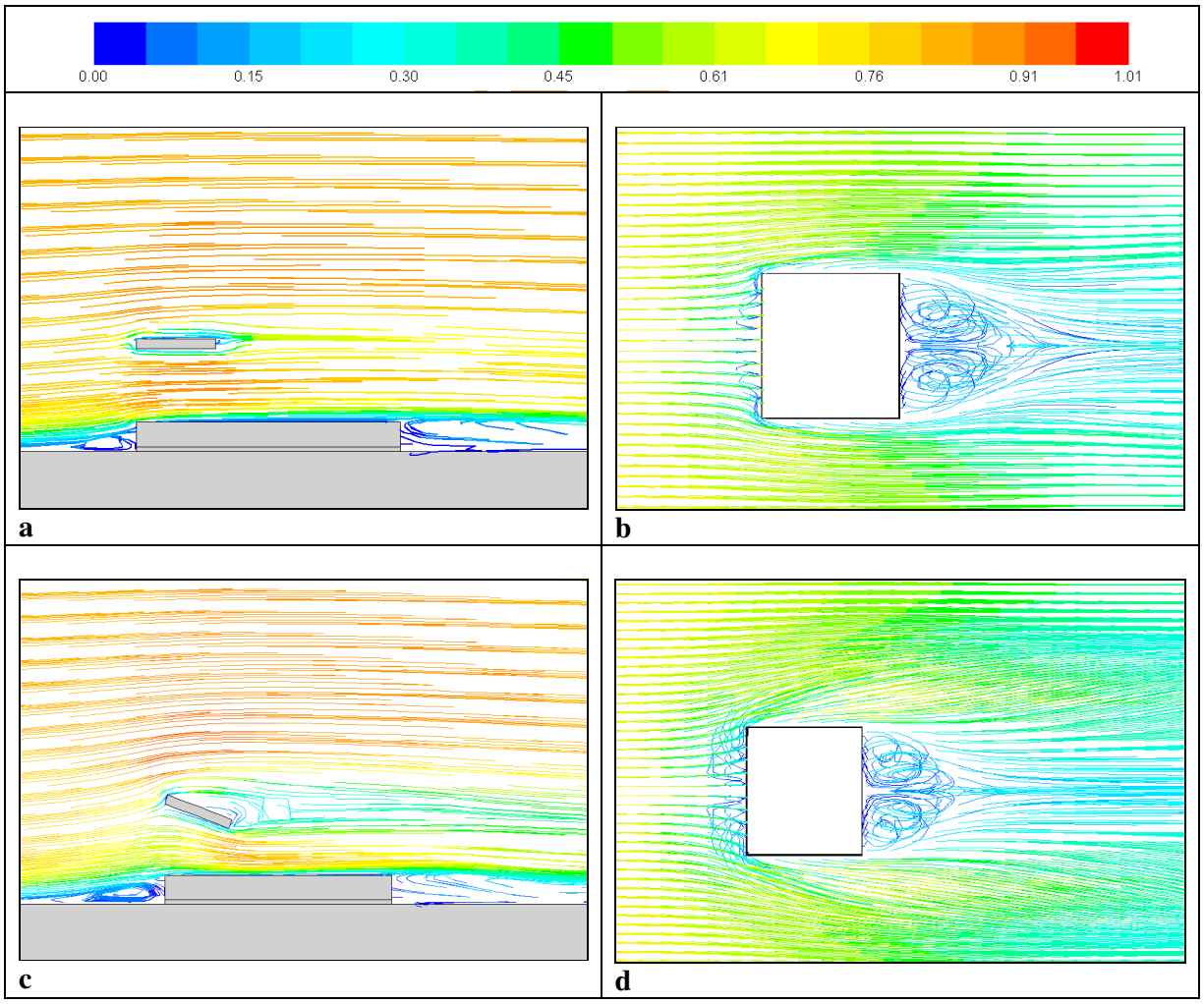

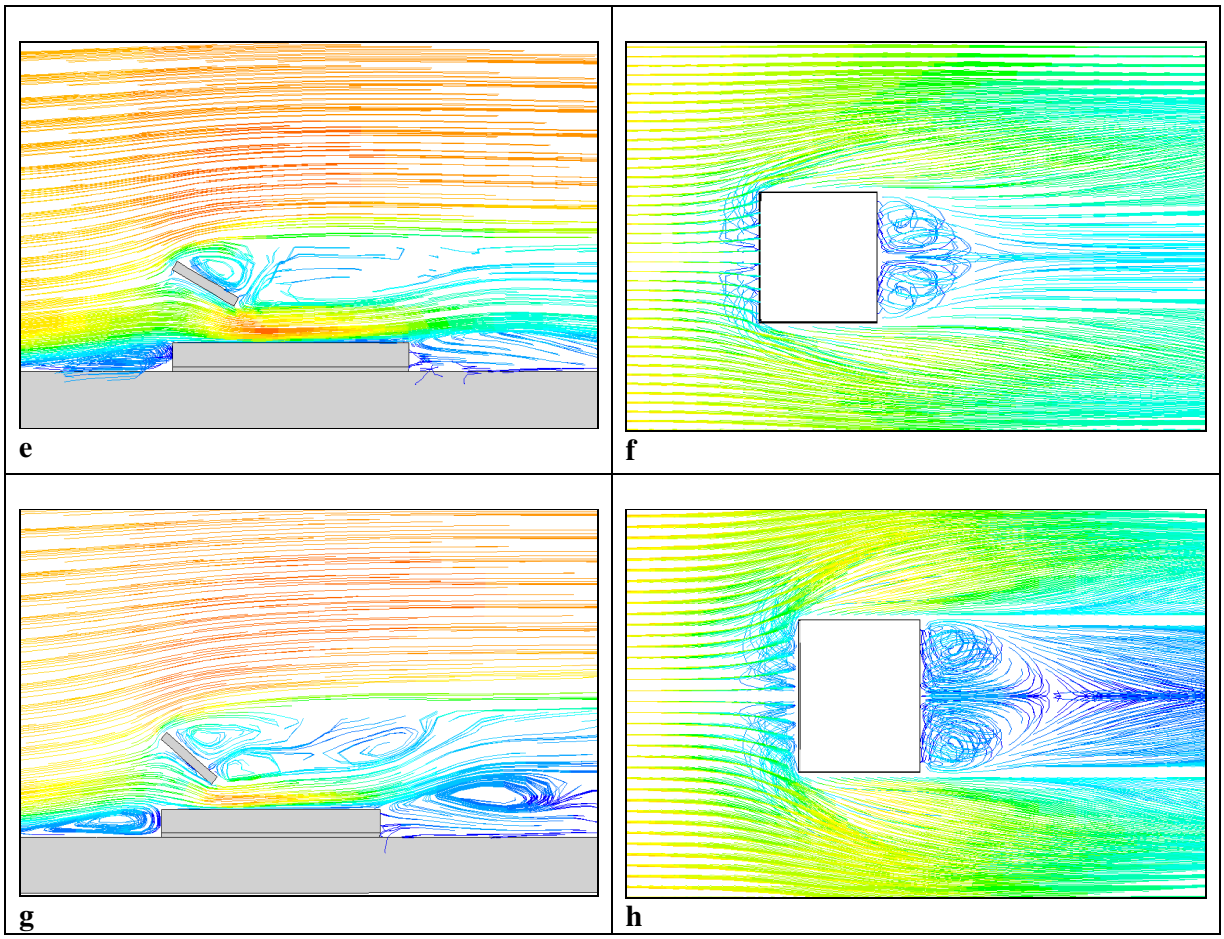

Figure 23: Streamline on z = 0 (figures a, c, e and g) and on y = -2 (figures b,d, f and h) with α =0° (**a, b**), α =20° (**c, d**) α =30° (**e, f**) and α =40° (**g, h**)

The streamlines show that small turbulent structures are located in the upstream corner. These smaller structures characterize upstream recirculation. We can note that it is more important when the inclination become important [Didarul, Oyakawa 2007]. The same thing is observed at downstream module. Actually, in case of α =40°, the recirculation become large. It must be noted that although the mean flow in symmetrical plane may be similar to 2D flow, outside of the symmetrical plane, the effect of the deflector, and the side of the heated bloc that is perpendicular to the mean stream is strongly felt, thus the flow becomes completely 3D. In addition, the path line demonstrate that the inclination angles have a strong influence on the shape of separated region on windward side of the module and it has also an influence on the recirculation region in the wake of the module (Figures 23: b, d, f and h).

Heat transfer coefficient The axial distributions of local heat transfer coefficients and the axial distributions of the surface temperature on the heated bloc are presented, for different inclination angle α, in Figures 24 and 25.

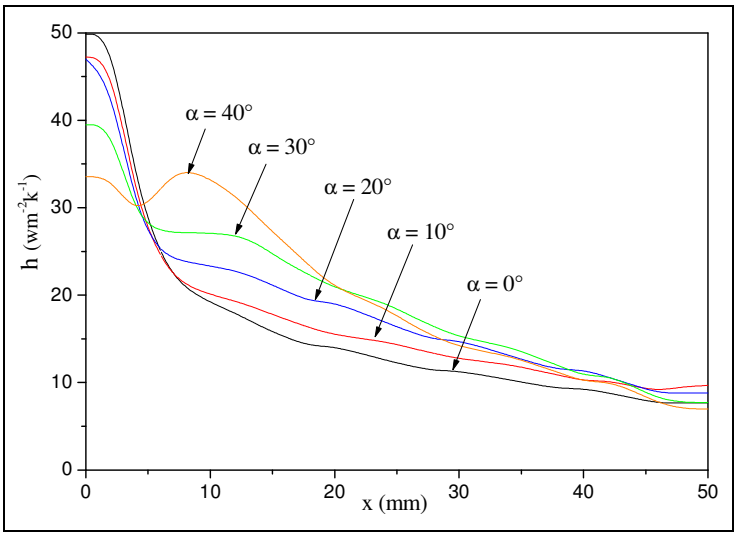

Figure 24: Comparison of local heat transfer coefficient at the midwidth of the bloc

A maximum of local heat coefficient is noted at x = 0 (h = 50 $Wm^{-2}k^{-1}$ in case of α =0°), we note a decrease of the local heat coefficient. However, in case of α =40°, the peak is located at x = 10 (h = 35 $Wm^{-2}k^{-1}$) before decreasing slowly. In addition, of α =40°, the local temperature is lower than the other cases (Figure 26).

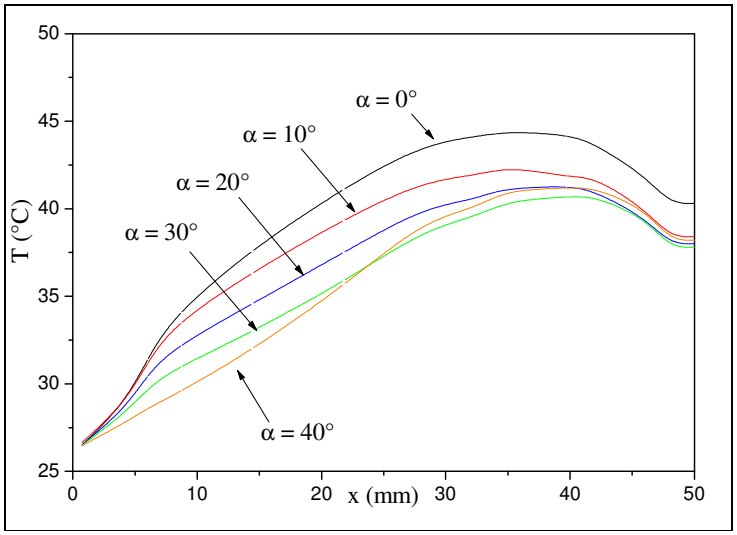

Figure 26: Comparison of local temperatures at midline for different α.

We found that the maximum heat transfer was obtained at an inclination angle of 40° (Table1). The deflections of flow induce the recirculation of air in the wake of the module and behind the deflector. These perturbations allow more extraction of heat from the surface of module and wake it.

Table 1
Comparison of heat transfer coefficient on the surface of module for different α

α (°)	without-deflector	0	10	20	30	40
h_{moy} (Wm^{-2} K^{-1})	15	17	18,5	19,5	20,5	22

Comparison of Numerical and experimental velocity Figures 26 and 27 show a comparison between the numerical and experimental investigations. In the case of α = 10°, we can note that the difference between numerical and experimental velocity is lower than 10 % except at x = 0, the difference is equal to 20 %. This is can be explain by two main reasons:

- First, it was considered important to indicate that the detachment from the wall is produced earlier in the numerical investigation. However, the reattachment of the flow predicted by the numerical simulation appears later than the one determined by the probe [Arts, Benicci, Rambaud 2007],.
- Second, the detachment, reattachment and recirculation of flow induce the change of direction of velocity vectors. Nevertheless, the probe determines the velocity by integrated the cooling air over the cylindrical surface of hot wire. For that reason, the velocity is overestimated in these regions.

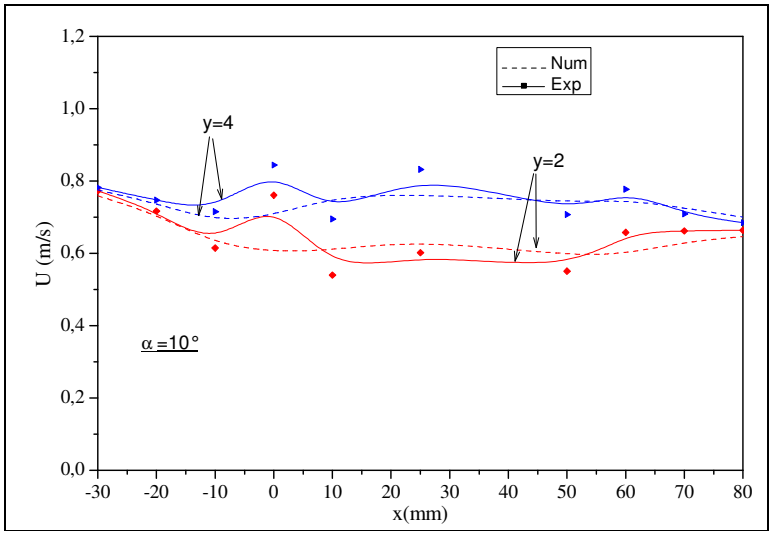

Figure 27 Comparison between numerical and experimental distribution of velocity at y = 2mm and at y = 4mm in cases of α = 10°,

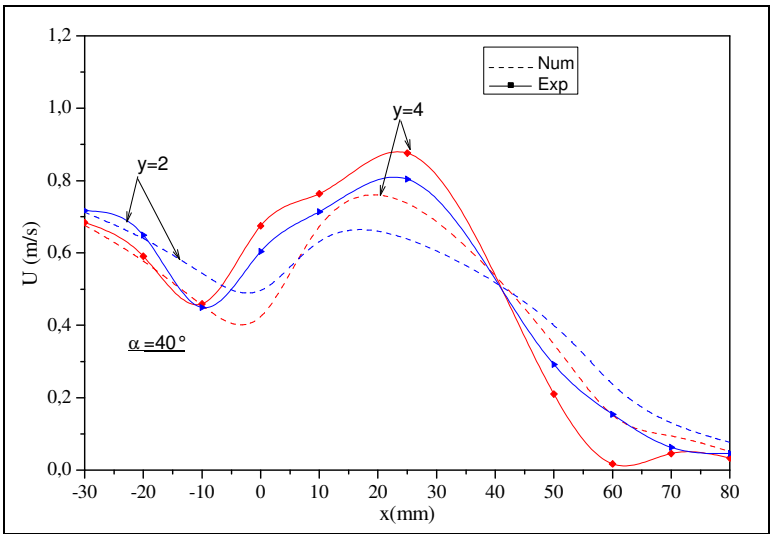

Figure 28 Comparison between numerical and experimental distribution of velocity at y = 2mm and at y = 4mm in cases of α = 40°,

Conclusion

The present paper combines experimental and numerical investigations of cooling hot electronic component with implementation of deflectors that guide the air flow to the upper surface of the component when there is no enough space to introduce heat sinks fins or a fan. The influence of deflectors and the inclination angle on enhancement of heat transfer have been investigated.
We have simulated this practical application by studying the flow pattern and the heat transfer on a heated rectangular bloc (50 mm * 50 mm) fixed on a flat PVC plate.
The thermal skewness and flatness factors show that the law governing the temperature fluctuations approximates the Gaussian law quite well in the region where an equal probability of the presence of the hot air coming from the module and the air flow is noted. Furthermore, the dynamic flatness and the skewness factors show that the law governing the velocity fluctuations approximates the Gaussian law. This behavior characterizes a high flowing of cold air arising from the ambient. However, a positive skewness factor characterizes the recirculation created by subdivision of flow in the above and under the deflector.
It has shown how numerical simulation can be used to complete the experimental investigation. The simulation makes in evidence the influence of deflectors and their inclination on the existence and importance of vortex structures in the flow (recirculation, detachment, reattachment…). Besides, it has proved their effect on enhancement of convective heat transfer.
The deflector trains flow to the hot module. The inclination of deflector allows extraction of higher heat flux from the module, whereas it exist an optimum inclination angle (a = 40°). A vortex was also observed but the strength of the vortex increase downstream the deflector when the inclination angle increases. Another phenomenon caused by deflecting is the recirculation of air in front of the module. This recirculation of air causes a decrease in velocity in this region and therefore an increase of temperature, whereas it gives higher value for the average heat transfer coefficient. It tends therefore to homogenize the temperature on the surface of the component, which is an important task in electronic cooling.

Acknowledgment
The authors would like to acknowledge the support of the Comité Mixte Franco-Tunisien pour la Coopération Universitaire (Project ; CMCU 08G1131).

REFERENCES

Kakaç S., Yurucu H., and Hijikata K.A. [1994], Cooling of Electronic Systems, *Kluwer Academic Publishers*.

Stewart T. and Stiver D. W. [2004], Thermal Optimization of Electronic Systems Using Design of Experiments Based on Numerical Inputs, *Proc. SEMI-THERM*, paper n°14

Kadangode Subha M., Mason John R. [2003], Optimization of Elliptical Fin Heat sink Design in Forced Convection: Single and Multiple Heat Sink, *Interpack,* Paper # 35029.

Zinoubi J, Ben Maad R, Belghith A. [2005], Experimental study of the resulting flow of plume–thermosiphon interaction: application to chimney problems. Appl Thermal Eng, 25:533–44.

Zinoubi J., Mahmoud A.O.M., Naffouti T., R.B. Maad and A. Belghith, [2006], Study of the flow structure of a thermal plume evolving in an unlimited and in a semi-enclosed environment. *Am. J. Appl*. Sci., 31: 1690-1697.

I.Md. Didarul et al [2007], Study on heat transfer and fluid flow characteristics with short rectangular plate fin of different patters, *Experimental Thermal and Fluid.* Sci., 31: 367-379.

Zhao Z [2003], Thermal design of a broadband communication system with detailed modeling of TBGA packages, *Microelectronics Reliability,* 785–793.

Arts T., Benicci C., Rambaud P. [2007], Experimental and Numerical Investigation of Flow and Heat Transfer in a Ribbed Square Duct, 3rd International Symposium on integrating CFD and Experiments in Aerodynamics, paper…